Rad51 filaments assembled in the absence of the complex formed by the Rad51 paralogs Rad55 and Rad57 are outcompeted by translesion DNA polymerases on UV-induced ssDNA gaps

Laurent Maloisel[1,*], Émilie Ma[1] and Éric Coïc[1,*]

[1]Université de Paris Cité and Université Paris-Saclay, Inserm, CEA IBFJ/iRCM, UMR Stabilité Génétique Cellules Souches et Radiations, F-92265, Fontenay-aux-Roses, France.

[*]Corresponding authors

E-mails: eric.coic@cea.fr; laurent.maloisel@cea.fr

Keywords: Rad51 paralogs, Rad55-Rad57, homologous recombination, translesion polymerases, Polζ, Polη.

Running title: Rad55-Rad57 prevents recruitment of translesion DNA polymerases

Abstract

The bypass of DNA lesions that block replicative polymerases during DNA replication relies on DNA damage tolerance pathways. The error-prone translesion synthesis (TLS) pathway relies on specialized DNA polymerases that incorporate nucleotides in front of base lesions, potentially inducing mutagenesis. Two error-free pathways can bypass the lesions: the template switching pathway, which uses the sister chromatid as a template, and the homologous recombination pathway (HR), which also can use the homologous chromosome as template. The balance between error-prone and error-free pathways controls the mutagenesis level. Therefore, it is crucial to precisely characterize factors that influence the pathway choice to better understand genetic stability at replication forks. In yeast, the complex formed by the Rad51 paralogs Rad55 and Rad57 promotes HR and template-switching at stalled replication forks. At DNA double-strand breaks (DSBs), this complex promotes Rad51 filament formation and stability, notably by counteracting the Srs2 anti-recombinase. To explore the role of the Rad55-Rad57 complex in error-free pathways, we monitored the genetic interactions between Rad55-Rad57, the translesion polymerases Polζ or Polη, and Srs2 following UV radiation that induces mostly single-strand DNA gaps. We found that the Rad55-Rad57 complex was involved in three ways. First, it protects Rad51 filaments from Srs2, as it does at DSBs. Second, it promotes Rad51 filament stability independently of Srs2. Finally, we observed that UV-induced HR is almost abolished in Rad55-Rad57 deficient cells, and is partially restored upon Polζ or Polη depletion. Hence, we propose that the Rad55-Rad57 complex is essential to promote Rad51 filament stability on single-strand DNA gaps, notably to counteract the error-prone TLS polymerases and mutagenesis.

47 # Author summary

48 Processive and accurate DNA polymerases replicate genomic DNA during the S phase of
49 each cell cycle. DNA base lesions on template DNA block these polymerases and result in an
50 accumulation of single-stranded DNA gaps behind moving replication forks. These gaps are
51 filled-in by error-prone and error-free pathways. In this work, we show that the complex made
52 by the Rad51 paralogs Rad55 and Rad57 is essential for the error-free homologous
53 recombination gap-filling pathway when DNA replication is stalled by UV-induced DNA
54 lesions, but not for DNA double strand break repair. Interestingly, we found that homologous
55 recombination is efficiently outcompeted by error-prone translesion DNA polymerases in
56 Rad55-Rad57-deficient cells. We propose that the Rad55-Rad57 complex is essential for
57 Rad51 filament stability at UV-induced DNA gaps to promote efficient error-free
58 homologous recombination. Furthermore, our study in yeast predicts that inhibitors of error-
59 prone DNA polymerases might selectively target cancer cells in which RAD51 paralogs are
60 mutated.

61

62 # Introduction

63 In all living organisms, genomic DNA undergoes chemical modifications or
64 crosslinking with proteins. These damages greatly compromise DNA replication because they
65 induce replication fork stalling. DNA damage tolerance mechanisms have evolved to ensure
66 completion of genome replication [1], and rely on two main mechanisms: i) translesion
67 synthesis (TLS) DNA polymerases and ii) the use of a homologous template, typically the
68 newly synthesized sister chromatid. Specialized TLS polymerases efficiently insert
69 nucleotides opposite and beyond lesions on DNA templates that block the replicative DNA
70 polymerases [2]. They possibly extend blocked primer/template junctions at replication forks
71 or at single-stranded DNA (ssDNA) gaps left behind the forks [3,4]. TLS polymerases are
72 intrinsically error-prone and constitute a major source of DNA damage-induced mutagenesis
73 [5,6]. Recombination-mediated pathways, such as the template switching and homologous
74 recombination (HR) pathways, mediate damage bypass through the annealing of the damaged
75 ssDNA gaps to the intact homologous template on the sister chromatid [7–9]. HR, also
76 referred to as the salvage pathway, can use homologous chromosomes as intact donors rather
77 than sister chromatids [10]. As TLS, template switching and HR compete for the same
78 ssDNA substrates, they can partly compensate for each other [11–13]. However, template
79 switching and HR are error-free lesion bypass mechanisms and counterbalance mutagenesis
80 induced by TLS [14,15]. Thus, it is crucial to precisely characterize the factors that influence
81 pathway choice to better understand genetic stability at replication forks.

82 The template switching pathway involves ubiquitin ligase and the Rad18/Rad6 pathway
83 conjugating activities. In budding yeast, Rad6 and Rad18 induce PCNA mono-ubiquitination
84 at its conserved K164 residue, whereas Rad5 and Mms2-Ubc13-dependent activities trigger
85 its poly-ubiquitination at K164 [16,17] and the formation of X-shaped intermediates between

86 sister chromatids when replication is challenged by DNA damages [8]. Interestingly, the
87 formation of these X-shaped intermediates relies also on the HR factors Rad51 and Rad52
88 [7,18].

89 The HR pathway relies on the recombinase Rad51 that oligomerizes on ssDNA to form
90 a right-handed helical nucleoprotein filament [19,20]. This filament performs homology
91 search and catalyzes DNA joint formation between ssDNA and double-stranded DNA
92 (dsDNA) homologous partners, thereby leading to strand exchange [21–23]. Eventually,
93 repair DNA synthesis occurs from the damaged DNA invading ends on undamaged template
94 homologous DNA sequences [24]. Rad51 loading on RPA-coated ssDNA is a crucial step in
95 HR and is mediated mainly by Rad52 in *Saccharomyces cerevisiae* and BRCA2 in metazoans
96 [25–27]. Rad51 filament assembly also requires the activity of Rad51 paralogs (Rad55-Rad57
97 complex in *S. cerevisiae*; RAD51B, RAD51C, RAD51D, XRCC2, and XRCC3 in human
98 cells; and the SHU complex in both [28]). Rad55 and Rad57 share 20% identity with the
99 RecA/Rad51 ATPase core region [29,30]. However, they do not form filaments on ssDNA,
100 and they do not exhibit strand exchange activity [31,32]. Electron microscopy images showed
101 the association of gold-labeled Rad55 with Rad51 filaments assembled on ssDNA (Rad51-
102 ssDNA) [32], and two-hybrid experiments revealed the interaction between Rad51 and Rad55
103 [33,34]. However, recent single-molecule studies suggest that the interaction between the
104 Rad55-Rad57 complex and Rad51 filaments is transient and the Rad55-Rad57 complex
105 dissociates during filament extension [35]. As similar findings were obtained in nematodes
106 [36], it has been proposed that RAD51 paralogs behave as classical chaperones to temporarily
107 assist Rad51 filament formation. More studies are required to clearly describe the precise role
108 of each complex of Rad51 paralogs. In addition, each complex might play a specific role
109 depending on the initial HR-inducing DNA lesion [37].

110 Rad55-Rad57 role in DNA double strand break (DSB) repair is considered accessory
111 on the basis of the weaker sensitivity of *rad55* and *rad57* mutants to ionizing radiation and to
112 site-directed DSBs compared with *rad51* mutants [38,39]. Interestingly, this sensitivity seems
113 to depend on the Srs2 helicase activity because it is partially suppressed by *SRS2* ablation
114 [32,39]. *In vitro* experiments have shown that the Srs2 translocase activity disrupts Rad51
115 filaments [40,41] and that the Rad55-Rad57 complex counteracts Srs2 to maintain Rad51
116 filaments on ssDNA [32,35]. Therefore, it has been proposed that Rad51 filament assembly
117 and disassembly, which are mediated by the Rad55-Rad57 complex and Srs2 respectively,
118 provide a regulatory mechanism to control HR initiation. However, *SRS2* deletion does not
119 rescue spontaneous HR defects between direct repeats in the *rad55* and *rad57* mutants,
120 indicating that the Rad55-Rad57 complex also acts independently of Srs2 [39].
121 To explain the different defects observed between spontaneous and DSB-induced HR,
122 it was hypothesized that spontaneous HR between direct repeats is initiated by ssDNA gaps
123 rather than DSBs [39]. Thus, the Rad55-Rad57 complex would play a more prominent role in
124 HR when the initiating lesion is a ssDNA gap. In agreement, it has been observed that in cells
125 lacking the TLS polymerases Pol ζ, *RAD55* ablation leads to a synergistic increase in DNA
126 damage sensitivity [42–44].
127 Here, we explored Rad55-Rad57 role in Rad51 filament formation on ssDNA gaps and
128 in the balance between HR and TLS in *S. cerevisiae*. For that purpose, we induced
129 interhomolog HR in diploid strains by ionizing radiation (IR) or UV radiation. IR generates
130 DSBs and ssDNA gaps, whereas UV generates mostly ssDNA gaps [11]. We found that the
131 Rad55-Rad57 complex is essential for UV-induced HR, but only accessory for IR-induced
132 HR. Interestingly, this essential role is mainly Srs2-independent, and UV-induced HR in
133 Rad55-Rad57-deficient cells can be restored by inactivation of a TLS polymerase (Polζ or
134 Polη). Conversely, UV-induced HR cannot be restored upon inactivation of the template

135 switch pathway in *MMS2* deficient cells. Overall, our results show that the Rad55-Rad57
136 complex is essential for Rad51 filament assembly on UV-induced ssDNA gaps. When this
137 complex is absent, Rad51 filaments cannot prevent the recruitment of TLS polymerases and
138 counterbalance mutagenesis.
139

140 Results

141 The Rad55-Rad57 heterodimer is essential for UV-induced 142 homologous recombination

143 To investigate Rad55-Rad57 role in HR induced by DSB and ssDNA gaps, we
144 analyzed UV- and IR-induced interhomolog HR in wild type (WT) and *rad55*Δ isogenic
145 diploid strains. The previous observation that *rad51* and *rad52* mutant cells are very sensitive
146 to IR indicates that IR generates DSBs, whereas these mutants are much more resistant to UV
147 radiation, indicating that DSBs are probably rarely induced [45,46]. Additionally, genetic
148 evidence suggests that UV-induced HR is triggered by ssDNA gaps [47]. We measured
149 interhomolog HR using two mutant alleles of *ARG4*: *arg4-RV*, a 2-bp deletion that ablates the
150 *Eco*RV site at position +258, and *arg4-Bg*, a 4-bp insertion by fill-in of a *Bgl*II site at position
151 +1,274 [48] (**Fig 1A**). These alleles do not revert [48] and only recombination in heteroallelic
152 *arg4-RV*/*arg4-Bg* diploid cells results in the formation of a WT *ARG4* gene primarily by non-
153 reciprocal transfer covering one mutation [49].
154 The *rad55*Δ diploid strain was not sensitive to UV radiation (**Fig 1B**), but remarkably,
155 UV-induced recombinant [Arg^+] frequency was strongly reduced in the *rad55*Δ diploid strain
156 compared with WT cells (10-fold at 120 J/m^2) (**Fig 1C**), suggesting that the Rad55-Rad57
157 complex is determinant in UV-induced HR. Conversely, *rad55*Δ diploid cells were sensitive
158 to IR (**Fig 1D**), but γ-ray-induced HR frequencies were identical in *rad55*Δ and WT cells at
159 high doses (400 Gy and 600 Gy) (**Fig 1E**). We observed the same phenotypes in the *rad57*Δ

160 mutant (**S1 Fig**). Likewise, it was previously reported that spontaneous HR rates are identical
161 in *rad57*Δ and WT cells [38,50], a result we confirmed here in *rad55*Δ cells (**Fig. 1F**). These
162 observations suggest that the Rad55-Rad57 complex plays a specific and essential role in UV-
163 induced HR, while it seems accessory for DSB repair induced by IR and spontaneous HR.
164

165 UV-induced DNA lesions are channeled towards the *REV3* 166 error-prone DNA repair pathway in the *rad55*Δ mutant

167 Although UV-induced HR was almost abolished in *rad55*Δ cells, these cells were
168 resistant to UV radiation. We hypothesized that in *rad55*Δ mutant cells, UV-induced ssDNA
169 gaps at replication forks could be repaired by TLS instead of HR. The TLS polymerase Polζ
170 is required to bypass UV-induced DNA lesions, as illustrated by the strong UV-sensitivity of
171 haploid cells lacking the Rev3 catalytic subunit of Polζ (**Fig 2A**) [51]. Conversely, *rev3*Δ
172 diploid cells were much more resistant to UV radiation (**Fig 2B**), possibly due to HR
173 promoted by *MAT* heterozygosity [50,52–54]. In addition, Polζ is responsible for almost all
174 UV-induced mutagenesis in yeast cells [51,55]. Therefore, we expected that *rad55*Δ cells
175 strongly rely on Polζ and on its catalytic subunit Rev3 for UV resistance, and that UV-
176 induced mutagenesis is increased in *rad55*Δ cells, as previously shown for spontaneous
177 mutagenesis [42]. In agreement with previous studies, we confirmed that UV sensitivity is
178 much higher in the *rev3*Δ *rad55*Δ double mutant than in the *rev3*Δ single mutant in haploid
179 cells [42–44] (**Fig 2A**) and also in diploid cells (**Fig 2B**). Therefore, the high resistance of
180 Rad55-deficient cells is related to the TLS pathway that could compensate for HR deficiency
181 in these cells.
182 We then monitored mutagenesis in *rad55*Δ cells using the *CAN1* forward mutation
183 assay [56]. In agreement with our hypothesis of a major role of the error-prone TLS pathway,
184 the frequency of UV-induced canavanine-resistant cells was two-fold higher in the *rad55*Δ

185 mutant than in WT cells (**Fig 2C**). This observation supports the channeling of DNA lesions
186 towards the error-prone Polζ-dependent pathway in *rad55*Δ cells.
187

188 UV-induced DNA lesions are channeled to the HR pathway 189 in cells lacking TLS polymerases

190 The finding that UV-induced DNA lesions can be channeled to the TLS pathway in
191 *rad55*Δ cells suggested that such lesions could be managed by the HR pathway in TLS-
192 deficient cells. In that case, TLS-deficient cells should display a hyper-recombinogenic
193 phenotype. To test this hypothesis, we measured the frequencies of UV-induced HR in *rev3*Δ
194 (Polζ mutant) and *rad30*Δ (Polη mutant) cells. As expected, HR frequency was strongly
195 increased in the *rev3*Δ and to a lower extent in the *rad30*Δ mutant (**Fig 3A and B**). However,
196 UV sensitivity was similar in diploid cells harboring the *rev3*Δ or *rad30*Δ mutation (**Figs 2B**
197 **and 3C**). We propose that in the *rad30*Δ mutant, UV-induced DNA lesions can be bypassed
198 by both HR and Polζ, while Polη cannot always take over Polζ function in *rev3*Δ cells,
199 resulting in higher HR frequency.
200

201 Translesion DNA polymerases prevent UV-induced HR in 202 the *rad55*Δ mutant

203 We showed that UV-induced HR is strongly decreased in Rad55-Rad57 deficient cells.
204 We also observed that the TLS and HR pathways compete for the same UV-induced ssDNA
205 gaps, because mutagenesis was increased in *rad55*Δ mutants, and HR in *rev3*Δ mutants.
206 Therefore, the recruitment of TLS polymerases at the lesion site might decrease HR in
207 *rad55*Δ cells. We measured HR frequencies in the *rev3*Δ *rad55*Δ double mutant, and
208 observed a significantly increased frequency compared with *rad55*Δ cells (**Fig 4A**). This
209 indicated that Polζ effectively impairs HR in the absence of the Rad55-Rad57 complex. We

210 propose that the Rad55-Rad57 complex is important to stabilize Rad51 filaments on ssDNA
211 gaps at the DNA lesion site, thus avoiding the recruitment of TLS polymerases. Our results
212 also suggest that in the absence of the Rad55-Rad57 complex, Rad51 filaments are functional
213 enough to promote some HR events (**Fig 4A**), but this is not sufficient to improve UV
214 resistance (**Fig 2**). We observed the same results when a Polη mutation (*rad30*Δ) was
215 combined with *rad55*Δ (**Fig 4B-D**). Thus, both Polζ and Polη are responsible for the decrease
216 of UV-induced HR in *rad55*Δ mutant cells.

217 Next, we asked whether UV-induced HR can be observed independently of the Rad55-
218 Rad57 complex in cells deficient for the template switching pathway. Therefore, we measured
219 the cell survival and recombination frequencies after UV radiation of cells in which *MMS2*
220 was deleted. We found that the *rad55*Δ *mms2*Δ double mutant was more sensitive than the
221 single mutants (**Fig 4E**), suggesting that some template switching events can occur
222 independently of HR. Strikingly, the frequency of UV-induced recombinants was very low in
223 the *rad55*Δ *mms2*Δ double mutant (**Fig 4F**). This suggests that the template switching
224 pathway does not compete with HR between homologous chromosome and that TLS
225 polymerases still prevent HR in the *rad55*Δ *mms2*Δ double mutant. On the other hand, the
226 recombination frequency in the *mms2*Δ single mutant was increased, but only after exposure
227 to the highest UV dose (120 J/m^2, **Fig 4F**).

228

229 The acute UV sensitivity of the *rad55*Δ *rev3*Δ double 230 mutant is partially suppressed by *SRS2* deletion

231 As the Rad55-Rad57 complex limits Rad51 filament destabilization by Srs2 at DSBs
232 [32,35], we asked whether Srs2 would be partially involved in the defective UV-induced HR
233 associated with *rad55*Δ or *rad57*Δ. To address this question, we measured UV-induced HR
234 frequencies in *rad55*Δ *srs2*Δ and *rad57*Δ *srs2*Δ double mutants. We found that they were

235 similar to those observed in *rad55*Δ and *rad57*Δ single mutants (**Fig 5A and 5B**; **S2A and**
236 **S2B Fig**). However, *rev3*Δ *rad55*Δ *srs2*Δ diploid cells were less sensitive to UV radiation
237 than *rev3*Δ *rad55*Δ cells (**Fig 5C**). Thus, the Rad55-Rad57 complex is involved also in the
238 protection of Rad51 filaments against Srs2 at ssDNA gaps formed after UV radiation, but this
239 can only be seen in the absence of Polζ. When Polζ is active, the HR rate is probably too low
240 in *rad55*Δ mutant cells to allow measuring the effect of Rad51 displacement by Srs2.
241 Additionally, despite Srs2 absence, the *rev3*Δ *rad55*Δ *srs2*Δ triple mutant was more
242 sensitive to UV than the *rev3*Δ single mutant (**Fig 5C**). This indicates that besides the
243 protection it provides to Rad51 filaments against Srs2, the Rad55-Rad57 complex plays a
244 Srs2-independent role in UV-induced HR that is only revealed in *rev3*Δ mutants. We propose
245 that the Rad55-Rad57 complex provides stability to Rad51 filaments independently of the
246 protection against Srs2.
247

248 The Rad55-Rad57 complex is essential for the formation of 249 UV-induced lethal recombination events

250 We confirmed that the *srs2*Δ/*srs2*Δ diploid strain is very sensitive to UV radiation as reported
251 before [57]; however, this sensitivity was completely suppressed in *rad55*Δ *srs2*Δ and
252 *rad57*Δ *srs2*Δ mutant cells (**Fig 5D**; **S2C Fig**). Previous genetic studies led to the concept of
253 toxic Rad51-dependent recombination intermediates that accumulate in the absence of Srs2
254 [58–60]. Therefore, on the basis of the complete suppression of *srs2*Δ-associated UV
255 sensitivity by *rad55*Δ and *rad57*Δ, we propose that the Rad55-Rad57 complex participates in
256 the formation of UV-induced Rad51 filaments that are toxic for the cells in the absence of
257 Srs2. In agreement with previous reports [57,61,62], we observed a strong UV-induced hyper-
258 recombination phenotype in Srs2-deficient cells. This phenotype was completely suppressed
259 by the concomitant deletion of Rad55 or Rad57 (**Fig 5A**; **S2A Fig**).

260

261 The translesion DNA polymerases Polζ and Polη are not 262 essential for DSB repair

263 The large impact of the *rad55*Δ *rev3*Δ double mutant on cell survival after UV radiation
264 suggested that the Rad55-Rad57 complex and Polζ play an important and specific role in UV-
265 induced DNA repair. Although the Rad55-Rad57 complex is not essential for DSB repair
266 [39], we wanted to determine the potential role of TLS polymerases in DSB repair in *rad55*Δ
267 cells. To this aim, we measured the repair of a DSB induced at the *MAT* locus upon
268 expression of the HO endonuclease controlled by a galactose-inducible promoter. The DSB
269 was repaired by HR using an ectopic *MAT***a**-inc sequence inserted in chromosome V [62,63]
270 (**Fig 6A**). After DSB induction, survival was decreased by 3-fold in *rad55*Δ cells compared
271 with WT cells (**Fig 6B**). Conversely, survival of the *rev3*Δ, *rad30*Δ, and *rev3*Δ *rad30*Δ
272 mutants was not affected by DSB induction, and they did not change the sensitivity of the
273 *rad55*Δ mutant. This indicates that the TLS polymerases are not required for DSB repair
274 efficiency.

275

276 Discussion

277 The Rad55-Rad57 complex is essential for HR-mediated 278 repair of UV-induced ssDNA gaps

279 Genetic studies provided evidence that ssDNA gaps are the major initiator of
280 spontaneous and UV-induced HR in yeast [47,57]. In addition, electron microscopy and two-
281 dimensional gel electrophoresis showed that UV-irradiated cells accumulate ssDNA gaps,
282 likely resulting from re-priming events downstream of stalled replication forks at UV-induced
283 DNA lesions [11]. UV-induced ssDNA gaps were also inferred from a physical assay [12]

284 and from the study of RPA focus distribution relatively to sites of ongoing replication [13].
285 Interestingly, both studies reported that TLS and HR counteract ssDNA gap accumulation.
286 Here, we show that the complex formed by the Rad51 paralogs Rad55 and Rad57 is
287 essential for Rad51 filament formation at UV-induced ssDNA gaps, while it is accessory for
288 Rad51 filament formation at DSB sites. We observed a strong decrease of HR frequencies in
289 the *rad55*Δ and *rad57*Δ mutants specifically after UV radiation. Moreover, we confirmed the
290 synergistic increase of UV sensitivity upon depletion of both Rad55 and Polζ in haploid and
291 diploid cells (Fig. 2A and B). We did not observe this negative interaction after induction of a
292 site-directed DSB (Fig. 6). In addition, we found that UV-induced mutagenesis at the *CAN1*
293 locus was increased in the *rad55*Δ mutant (Fig. 2C), and that UV-induced HR was increased
294 in Pol ζ and Pol η deficient cells (Fig. 3A and B). Most importantly, we observed UV-
295 induced HR in the absence of the Rad55-Rad57 complex only in cells deficient for TLS (Fig.
296 4). These data suggest that the Rad55-Rad57 complex might stabilize Rad51 filaments on
297 ssDNA gaps to prevent the recruitment of the TLS polymerases.
298

299 The Rad55-Rad57 complex plays three prominent roles in 300 UV-induced HR

301 One of the best defined role of Rad55-Rad57 is the protection of Rad51 filaments from
302 Srs2 at DSBs [32,35]. Here, we found that although the defect in UV-induced HR observed in
303 *rad55*Δ cells was not suppressed by *SRS2* deletion **(Fig 5A and B)**, the very high UV
304 sensitivity of the *rad55*Δ *rev3*Δ double mutant was partially suppressed by *srs2*Δ (**Fig 5C**).
305 This suggests that the Rad55-Rad57 complex protects Rad51 filaments against Srs2 also at
306 UV-induced ssDNA gaps, although Esc2- and Elg1-dependent mechanisms also regulate
307 negatively Srs2 at sites of stalled replication forks [64,65]. More genetic studies are required
308 to determine the interplay between these regulating factors.

309 The increased UV-sensitivity of the *rev3*Δ *rad55*Δ *srs2*Δ triple mutant compared with
310 the *rev3*Δ single mutant (**Fig 5C**) clearly indicates that the Rad55-Rad57 complex plays a
311 Srs2-independent role in UV-induced HR. We propose that the second role of this complex is
312 to provide stability to Rad51 filaments, independently of the protection against Srs2. In
313 agreement with this conclusion, we found that in *rad55*Δ or *rad57*Δ mutants, *srs2*Δ-
314 associated UV-sensitivity was completely suppressed (**Fig 5D, S2C Fig**). This indicates that
315 in the absence of Srs2 activity, Rad51 stabilization by the Rad55-Rad57 complex would lead
316 to lethal events, possibly initiated by ssDNA gaps that could block replication fork restart. On
317 the basis of the results of single-molecule studies, it was proposed that the Rad55-Rad57
318 complex helps Rad51 filament formation by acting as a chaperone [35], in agreement with our
319 observations.
320 Remarkably, UV-induced HR frequency increased in *rad55*Δ cells upon Polζ or Polη
321 deletion (**Fig 5**). Therefore, the third role of the Rad55-Rad57 complex would be to allow HR
322 to outcompete the TLS polymerases. Rad51 filament stabilization by the Rad55-Rad57
323 complex on ssDNA at the lesion site could prevent the recruitment of TLS polymerases by
324 PCNA because of structural constraints. In the absence of Rad55-Rad57, unstable Rad51
325 filaments cannot prevent the loading of the TLS polymerases that inhibit HR and induce
326 mutagenesis. TLS polymerase depletion in *rad55*Δ mutants would allow some HR events to
327 occur, but the inherent instability of Rad51 filaments would make them rare and explain the
328 low survival rate of *rev3*Δ *rad55*Δ mutant cells. Our results clearly highlight that UV-induced
329 lesions can be channeled from HR to TLS and *vice versa*, when one pathway is inactivated.
330 This provide further support to a model in which HR and TLS can share common substrates
331 [12,13].
332

333 ## Model for the activity of the Rad55-Rad57 complex in
334 ssDNA gap repair

335 Our genetic data suggest three different and essential functions for the Rad55-Rad57
336 complex in UV-induced interhomolog HR initiated at ssDNA gaps (**Fig 7A**). First, this
337 complex is required for Rad51 filament formation and stabilization that are essential for
338 efficient strand exchange at ssDNA gaps. The 5'ends of DSBs are resected to generate 3'
339 ssDNA that can invade the homologous donor. Conversely, 3' ssDNA is not directly available
340 at ssDNA gaps. Therefore, the Rad55-Rad57 complex may be required to form Rad51
341 filaments that can invade without 3' ssDNA extremities. Alternatively, the Rad55-Rad57
342 complex can be involved in the 3' end denaturation at the lesion site to generate a 3' ended
343 ssDNA by recruitment of a DNA helicase. Second, the Rad55-Rad57 complex within Rad51
344 filaments counterbalances Srs2 activity through a mechanism that remains poorly understood
345 [32,35]. Third, the Rad55-Rad57 complex inhibits TLS polymerases by preventing their
346 loading at the primer/template junction within ssDNA gaps, probably through the stabilization
347 of Rad51 filaments (**Fig 7B-E**). This competition might be crucial to control mutagenesis
348 resulting from gap-filling by Polζ. Thus, in our model, Rad51 filaments formed with the
349 Rad55-Rad57 complex preserve the genome stability through ssDNA gap repair by HR, but
350 also through direct competition with TLS on common ssDNA gap substrates.
351

352 ## The interplay between HR and TLS in mammals

353 The interplay between error-prone and error-free lesion-bypass pathways is documented
354 in *E. coli* and yeast (the present study, [13,14]), and it has been recently investigated in
355 mammals. Specifically, in mammalian cells, HR is triggered by PRIMPOL-dependent ssDNA
356 gaps behind stalled replication forks [66]. Moreover, BRCA1- and BRCA2-defective breast
357 cancer cells, in which HR is impaired, display an increased somatic mutational load specific

358 of TLS polymerases [67–70]. Accordingly, a recent study found that BRCA1/2-defective
359 cancer cells rely much more on TLS for repair of PRIMPOL-dependent ssDNA gaps [71]. In
360 addition, similarly to PARP1 or DNA polymerase Polθ inhibitors that are used to treat HR-
361 deficient cancers [72–74], the small molecule JE-RH-06 disrupts the interaction between the
362 TLS polymerases REV1 and Polζ and shows preferential cytotoxicity in BRCA1-deficient
363 cancer cells [71,75]. Thus, it would be interesting to determine whether the association of
364 cancer-associated RAD51 paralog mutations and TLS mutations leads to a synergic
365 sensitivity to replication fork blocking lesions, as we observed in yeast in the *rad55*Δ *rev3*Δ
366 double mutant. If an acute sensitivity is found, one might expect a cytotoxicity associated
367 with TLS polymerase inhibitors in RAD51 paralog-deficient cancer cells.

368 # Materials and Methods

369 ## Yeast strains, plasmids and media

370 The *S. cerevisiae* strains used in the present study are isogenic derivatives of FF18733
371 (*his7-2, leu2-3,112, lys1-1, trp1-289, ura3-52*) and JKM146 (*hml::ADE1 MATalpha*
372 *hmr::ADE1*, *arg5,6::MATa-inc::HPH1*, *ade3::GAL::HO*) and are listed in **S1 Table**. Yeast
373 cells were incubated at 30°C for all the experiments described. Gene deletions were
374 performed by PCR-mediated one-step replacement [76,77]. Mutants were selected on YPD
375 medium containing 300 mg/L geneticin (Sigma) or nourseothricin (cloNAT; Werner
376 BioAgents). All deletions were confirmed by PCR amplification of genomic DNA. All media
377 were prepared as previously described [78].
378

379 ## Irradiation, cell survival assay, and measurement of DNA
380 ## damage-induced HR frequency

381 Cells in stationary phase and in exponential growth phase were used for irradiation
382 with UV and γ-rays, respectively. UV irradiation was performed using a 264 nm source.
383 Yeast cells were irradiated with 30, 60, 90 and 120 J/m^2 (2 J/m^2/s dose rate). γ-irradiation was
384 performed using a GSR D1 irradiator (Gamma-Service Medical GmbH). It is a self-shielded
385 irradiator with four sources of ^{137}Cesium. The total activity was 180.28 TBq in March 2014.
386 As yeast cells resuspended in 1 mL of sterile H_2O were irradiated in 1.5ml plastic microtubes,
387 dosimetry was performed using plastic microtubes with a cylindrical ionizing chamber 31010
388 (PTW, Freiburg, Germany) following the American Association of Physicists in Medicine
389 recommendations [79]. This ionizing chamber has a cavity of 0.125 cm^3 calibrated with
390 ^{137}Cesium in air kerma free in air and the reference number of our facility is 210382401. The
391 polarity and the ion recombination were measured for this ^{137}Cesium source. Each

392 measurement was corrected with the KTP factor to take into account the variations in
393 temperature and atmospheric pressure. Yeast cells were irradiated at 100, 200, 400 and 600
394 Gy (single doses) and with a 12 Gy/min dose rate that takes the radioactive decrease into
395 account.

396 Before (UV) or after (γ-rays) irradiation, cells were plated at the appropriate dilution
397 on rich medium (YPD) to measure the survival rate, and on synthetic plates without arginine
398 to quantify the number of HR events between *ARG4* heteroalleles. HR frequencies were
399 determined by dividing the number of recombinant colonies growing on selective medium by
400 the number of unselected colonies subjected to the same dose of irradiation. The values
401 obtained were corrected by subtracting the number of recombinants on the non-irradiated
402 plates. The mean percentage from at least three independent experiments is presented.
403

404 Measurement of spontaneous heteroallelic HR

405 Rates of spontaneous HR between two heteroalleles of *ARG4* were determined by
406 fluctuation tests using the method of the median [80]. The reported rates were obtained from
407 three independent experiments, each performed with nine independent 2-ml cultures started
408 with less than 200 cells and incubated at 30°C for three days. The significance of the rates is
409 indicated by the 95% confidence interval [80].
410

411 Measurement of UV-induced mutagenesis

412 UV-induced mutagenesis was measured with the *CAN1* forward-mutation assay [56].
413 UV-induced mutagenesis frequencies were obtained by dividing the number of colonies
414 growing on synthetic plates without arginine and containing l-canavanine (Sigma, 30 mg/l)
415 (*i.e.*, canavanine-resistant, Can^R, cells) by the number of cells that survived irradiation
416 counted on rich media YPD. The number of Can^R colonies obtained after irradiation was

417 corrected by subtracting the number of spontaneous Can^R colonies growing on non-irradiated
418 plates.
419

420 Survival following DSB formation

421 Cells were grown overnight in liquid culture medium containing lactate acid instead of
422 glucose. Survival following HO-induced DSB was measured as the number of cells growing
423 on galactose-containing medium divided by the number of colonies growing on YPD. The
424 results shown are the mean values of at least 3 independent experiments.
425

426 Acknowledgments

427 We thank Jim Haber, Pablo Radicella, Stéphane Marcand and Stefano Mattarocci for critical
428 and careful reading of the manuscript. We thank Véronique Ménard from the radiation facility
429 of our institute for her help with the use of the GSRD1 irradiator. We also appreciate the help
430 of Elisabetta Andermarcher with the English editing.
431

432 References

433 1. Branzei D, Psakhye I. DNA damage tolerance. Curr Opin Cell Biol. 2016;40: 137–144.
434 doi:https://doi.org/10.1016/j.ceb.2016.03.015
435 2. Zhao L, Todd Washington M. Translesion synthesis: Insights into the selection and
436 switching of DNA polymerases. Genes. 2017. doi:10.3390/genes8010024
437 3. Lehmann AR, Fuchs RP. Gaps and forks in DNA replication: Rediscovering old
438 models. DNA Repair (Amst). 2006;5: 1495–1498. doi:10.1016/j.dnarep.2006.07.002
439 4. Hedglin M, Benkovic SJ. Eukaryotic Translesion DNA Synthesis on the Leading and
440 Lagging Strands: Unique Detours around the Same Obstacle. Chemical Reviews. 2017.

441 doi:10.1021/acs.chemrev.7b00046

442 5. Waters LS, Minesinger BK, Wiltrout ME, D'Souza S, Woodruff R V, Walker GC.
443 Eukaryotic translesion polymerases and their roles and regulation in DNA damage
444 tolerance. Microbiol Mol Biol Rev. 2009;73: 134–154. doi:10.1128/MMBR.00034-08

445 6. Makarova A V, Stodola JL, Burgers PM. A four-subunit DNA polymerase ζ complex
446 containing Pol δ accessory subunits is essential for PCNA-mediated mutagenesis.
447 Nucleic Acids Res. 2012;40: 11618–11626. doi:10.1093/nar/gks948

448 7. Liberi G, Maffioletti G, Lucca C, Chiolo I, Baryshnikova A, Cotta-Ramusino C, et al.
449 Rad51-dependent DNA structures accumulate at damaged replication forks in sgs1
450 mutants defective in the yeast ortholog of BLM RecQ helicase. Genes Dev. 2005;19:
451 339–350. doi:10.1101/gad.322605

452 8. Branzei D, Vanoli F, Foiani M. SUMOylation regulates Rad18-mediated template
453 switch. Nature. 2008. pp. 915–920. doi:10.1038/nature07587

454 9. Branzei D, Szakal B. DNA damage tolerance by recombination: Molecular pathways
455 and DNA structures. DNA Repair (Amst). 2016;44: 68–75.
456 doi:10.1016/j.dnarep.2016.05.008

457 10. Carr AM, Lambert S. Replication stress-induced genome instability: The dark side of
458 replication maintenance by homologous recombination. Journal of Molecular Biology.
459 2013. pp. 4733–4744. doi:10.1016/j.jmb.2013.04.023

460 11. Lopes M, Foiani M, Sogo JM. Multiple mechanisms control chromosome integrity
461 after replication fork uncoupling and restart at irreparable UV lesions. Mol Cell.
462 2006;21: 15–27. doi:10.1016/j.molcel.2005.11.015

463 12. Ma W, Westmoreland JW, Resnick MA. Homologous recombination rescues ssDNA
464 gaps generated by nucleotide excision repair and reduced translesion DNA synthesis in
465 yeast G2 cells. Proc Natl Acad Sci U S A. 2013;110. doi:10.1073/pnas.1301676110

466 13. Wong RP, García-Rodríguez N, Zilio N, Hanulová M, Ulrich HD. Processing of DNA
467 Polymerase-Blocking Lesions during Genome Replication Is Spatially and Temporally
468 Segregated from Replication Forks. Mol Cell. 2020;77: 3-16.e4.
469 doi:10.1016/j.molcel.2019.09.015
470 14. Fujii S, Isogawa A, Fuchs RP. Chronological switch from translesion synthesis to
471 homology- Dependent gap repair in vivo. Toxicol Res. 2018;34: 297–302.
472 doi:10.5487/TR.2018.34.4.297
473 15. Masłowska KH, Laureti L, Pagès V. iDamage: a method to integrate modified DNA
474 into the yeast genome. Nucleic Acids Res. 2019;47: e124. doi:10.1093/nar/gkz723
475 16. Hoege C, Pfander B, Moldovan G-L, Pyrowolakis G, Jentsch S. RAD6-dependent
476 DNA repair is linked to modification of PCNA by ubiquitin and SUMO. Nature.
477 2002;419: 135–141. doi:10.1038/nature00991
478 17. Torres-Ramos CA, Prakash S, Prakash L. Requirement of RAD5 and MMS2 for
479 Postreplication Repair of UV-Damaged DNA in Saccharomyces cerevisiae. Mol Cell
480 Biol. 2002;22: 2419–2426. doi:10.1128/MCB.22.7.2419-2426.2002
481 18. Vanoli F, Fumasoni M, Szakal B, Maloisel L, Branzei D. Replication and
482 recombination factors contributing to recombination-dependent bypass of DNA lesions
483 by template switch. PLoS Genet. 2010;6: e1001205. doi:10.1371/journal.pgen.1001205
484 19. Conway AB, Lynch TW, Zhang Y, Fortin GS, Fung CW, Symington LS, et al. Crystal
485 structure of a Rad51 filament. Nat Struct Mol Biol. 2004;11: 791–796.
486 doi:10.1038/nsmb795
487 20. Short JM, Liu Y, Chen S, Soni N, Madhusudhan MS, Shivji MKK, et al. High-
488 resolution structure of the presynaptic RAD51 filament on single-stranded DNA by
489 electron cryo-microscopy. Nucleic Acids Res. 2016;44: 9017–9030.
490 doi:10.1093/nar/gkw783

491 21. San Filippo J, Sung P, Klein H. Mechanism of eukaryotic homologous recombination.
492 Annu Rev Biochem. 2008;77: 229–257.
493 doi:10.1146/annurev.biochem.77.061306.125255
494 22. Bell JC, Kowalczykowski SC. Mechanics and Single-Molecule Interrogation of DNA
495 Recombination. Annu Rev Biochem. 2016;85: 193–226. doi:10.1146/annurev-
496 biochem-060614-034352
497 23. Haber JE. DNA Repair: The Search for Homology. BioEssays. 2018.
498 doi:10.1002/bies.201700229
499 24. Mehta A, Haber JE. Sources of DNA double-strand breaks and models of
500 recombinational DNA repair. Cold Spring Harb Perspect Biol. 2014;6: a016428.
501 doi:10.1101/cshperspect.a016428
502 25. Sung P. Function of yeast Rad52 protein as a mediator between replication protein A
503 and the Rad51 recombinase. J Biol Chem. 1997;272: 28194–28197.
504 doi:10.1074/jbc.272.45.28194
505 26. Mortensen UH, Lisby M, Rothstein R. Rad52. Current Biology. 2009.
506 doi:10.1016/j.cub.2009.06.001
507 27. Carver A, Zhang X. Rad51 filament dynamics and its antagonistic modulators. Semin
508 Cell Dev Biol. 2021;113: 3–13. doi:10.1016/j.semcdb.2020.06.012
509 28. Bonilla B, Hengel SR, Grundy MK, Bernstein KA. RAD51 Gene Family Structure and
510 Function. Annu Rev Genet. Annual Reviews; 2020;54: 25–46. doi:10.1146/annurev-
511 genet-021920-092410
512 29. Kans JA, Mortimer RK. Nucleotide sequence of the RAD57 gene of Saccharomyces
513 cerevisiae. Gene. 1991;105: 139–140. doi:https://doi.org/10.1016/0378-
514 1119(91)90527-I
515 30. Lovett ST. Sequence of the RAD55 gene of Saccharomyces cerevisiae: similarity of

516 RAD55 to prokaryotic RecA and other RecA-like proteins. Gene. 1994;
517 doi:10.1016/0378-1119(94)90362-X
518 31. Sung P. Yeast Rad55 and Rad57 proteins form a heterodimer that functions with
519 replication protein A to promote DNA strand exchange by Rad51 recombinase. Genes
520 Dev. 1997;11: 1111–1121. doi:10.1101/gad.11.9.1111
521 32. Liu J, Renault L, Veaute X, Fabre F, Stahlberg H, Heyer W-D. Rad51 paralogues
522 Rad55–Rad57 balance the antirecombinase Srs2 in Rad51 filament formation. Nature.
523 2011;479: 245–248. doi:10.1038/nature10522
524 33. Hays SL, Firmenich AA, Berg P. Complex formation in yeast double-strand break
525 repair: Participation of Rad51, Rad52, Rad55, and Rad57 proteins. Proc Natl Acad Sci
526 U S A. 1995;92: 6925–6929. doi:10.1073/pnas.92.15.6925
527 34. Johnson RD, Symington LS. Functional differences and interactions among the
528 putative RecA homologs Rad51, Rad55, and Rad57. Mol Cell Biol. 1995;15: 4843–
529 4850. doi:10.1128/MCB.15.9.4843
530 35. Roy U, Kwon Y, Marie L, Symington L, Sung P, Lisby M, et al. The Rad51 paralog
531 complex Rad55-Rad57 acts as a molecular chaperone during homologous
532 recombination. Mol Cell. 2021;81: 1043-1057.e8. doi:10.1016/j.molcel.2020.12.019
533 36. Belan O, Barroso C, Kaczmarczyk A, Anand R, Federico S, O'Reilly N, et al. Single-
534 molecule analysis reveals cooperative stimulation of Rad51 filament nucleation and
535 growth by mediator proteins. Mol Cell. 2021;81: 1058-1073.e7.
536 doi:10.1016/j.molcel.2020.12.020
537 37. Garcin EB, Gon S, Sullivan MR, Brunette GJ, de Cian A, Concordet JP, et al.
538 Differential requirements for the RAD51 paralogs in genome repair and maintenance in
539 human cells. PLoS Genet. 2019;15: 1–29. doi:10.1371/journal.pgen.1008355
540 38. Mozlin AM, Fung CW, Symington LS. Role of the Saccharomyces cerevisiae Rad51

541 paralogs in sister chromatid recombination. Genetics. 2008;178: 113–125.
542 doi:10.1534/genetics.107.082677
543 39. Fung CW, Mozlin AM, Symington LS. Suppression of the double-strand-break-repair
544 defect of the Saccharomyces cerevisiae rad57 mutant. Genetics. 2009;181: 1195–1206.
545 doi:10.1534/genetics.109.100842
546 40. Veaute X, Jeusset J, Soustelle C, Kowalczykowski SC, Le Cam E, Fabre F. The Srs2
547 helicase prevents recombination by disrupting Rad51 nucleoprotein filaments. Nature.
548 2003;423: 309–312. doi:10.1038/nature01585
549 41. Krejci L, Van Komen S, Li Y, Villemain J, Reddy MS, Klein H, et al. DNA helicase
550 Srs2 disrupts the Rad51 presynaptic filament. Nature. 2003;423: 305–309.
551 42. Xu X, Ball L, Chen W, Tian X, Lambrecht A, Hanna M, et al. The yeast Shu complex
552 utilizes homologous recombination machinery for error-free lesion bypass via physical
553 interaction with a Rad51 paralogue. PLoS One. 2013;8: 1–9.
554 doi:10.1371/journal.pone.0081371
555 43. Rattray AJ, Shafer BK, McGill CB, Strathern JN. The roles of REV3 and RAD57 in
556 double-strand-break-repair-induced mutagenesis of Saccharomyces cerevisiae.
557 Genetics. 2002;162: 1063–1077.
558 44. Ball LG, Zhang K, Cobb JA, Boone C, Xiao W. The yeast Shu complex couples error-
559 free post-replication repair to homologous recombination. Mol Microbiol. 2009;73:
560 89–102. doi:10.1111/j.1365-2958.2009.06748.x
561 45. Chanet R, Heude M, Adjiri a, Maloisel L, Fabre F. Semidominant mutations in the
562 yeast Rad51 protein and their relationships with the Srs2 helicase. Mol Cell Biol.
563 1996;16: 4782–9. Available:
564 http://www.pubmedcentral.nih.gov/articlerender.fcgi?artid=231479&tool=pmcentrez&
565 rendertype=abstract

566 46. Game JC, Mortimer RK. A genetic study of X-ray sensitive mutants in yeast. Mutat
567 Res - Fundam Mol Mech Mutagen. 1974; doi:10.1016/0027-5107(74)90176-6
568 47. Lettier G, Feng Q, De Mayolo AA, Erdeniz N, Reid RJD, Lisby M, et al. The role of
569 DNA double-strand breaks in spontaneous homologous recombination in S. cerevisiae.
570 PLoS Genet. 2006;2: 1773–1786. doi:10.1371/journal.pgen.0020194
571 48. Coïc E, Gluck L, Fabre F. Evidence for short-patch mismatch repair in Saccharomyces
572 cerevisiae. EMBO J. 2000; doi:10.1093/emboj/19.13.3408
573 49. Petes T. 8 Recombination in Yeast. Cold Spring Harbor …. 1991.
574 50. Friis J, Roman H. The effect of the mating-type alleles on intragenic recombination in
575 yeast. Genetics. 1968;
576 51. Lemontt JF. Pathways of ultraviolet mutability in Saccharomyces cerevisiae. I. Some
577 properties of double mutants involving uvs9 and rev. Mutat Res - Fundam Mol Mech
578 Mutagen. 1971; doi:10.1016/0027-5107(71)90041-8
579 52. Lovett ST, Mortimer RK. Characterization of null mutants of the RAD55 gene of
580 Saccharomyces cerevisiae: effects of temperature, osmotic strength and mating type.
581 Genetics. 1987;
582 53. Heude M, Fabre F. a/α-control of DNA repair in the yeast Saccharomyces cerevisiae:
583 Genetic and physiological aspects. Genetics. 1993;
584 54. Valencia-Burton M, Oki M, Johnson J, Seier TA, Kamakaka R, Haber JE. Different
585 mating-type-regulated genes affect the DNA repair defects of saccharomyces RAD51,
586 RAD52 and RAD55 mutants. Genetics. 2006; doi:10.1534/genetics.106.058685
587 55. Quah SK, Von Borstel RC, Hastings PJ. The origin of spontaneous mutation in
588 Saccharomyces cerevisiae. Genetics. 1980; doi:10.1093/genetics/96.4.819
589 56. Whelan WL, Gocke E, Manney TR. The CAN1 locus of Saccharomyces cerevisiae:
590 Fine-structure analysis and forward mutation rates. Genetics. 1979;

591 doi:10.1093/genetics/91.1.35
592 57. Aboussekhra A, Chanet R, Zgaga Z, Cassier-Chauvat C, Heude M, Fabre F. RADH, a
593 gene of Saccharomyces cerevisiae encoding a putative DNA helicase involved in DNA
594 repair. Characteristics of radH mutants and sequence of the gene. Nucleic Acids Res.
595 1989; doi:10.1093/nar/17.18.7211
596 58. Gangloff S, Soustelle C, Fabre F. Homologous recombination is responsible for cell
597 death in the absence of the Sgs1 and Srs2 helicases. Nat Genet. 2000;25: 192–194.
598 doi:10.1038/76055
599 59. Klein HL. Mutations in recombinational repair and in checkpoint control genes
600 suppress the lethal combination of srs2Δ with other DNA repair genes in
601 Saccharomycescerevisiae. Genetics. 2001;157: 557–565.
602 60. Fabre F, Chan A, Heyer WD, Gangloff S. Alternate pathways involving Sgs1/Top3,
603 Mus81/ Mms4, and Srs2 prevent formation of toxic recombination intermediates from
604 single-stranded gaps created by DNA replication. Proc Natl Acad Sci U S A. 2002;99:
605 16887–16892. doi:10.1073/pnas.252652399
606 61. Rong L, Palladino F, Aguilera A, Klein HL. The hyper-gene conversion hpr5-1
607 mutation of Saccharomyces cerevisiae is an allele of the SRS2/RADH gene. Genetics.
608 1991;127: 75 LP – 85. Available: http://www.genetics.org/content/127/1/75.abstract
609 62. Esta A, Ma E, Dupaigne P, Maloisel L, Guerois R, Le Cam E, et al. Rad52 sumoylation
610 prevents the toxicity of unproductive Rad51 filaments independently of the anti-
611 recombinase Srs2. PLoS Genet. 2013;9: e1003833. doi:10.1371/journal.pgen.1003833
612 63. Ira G, Malkova A, Liberi G, Foiani M, Haber JE. Srs2 and Sgs1-Top3 suppress
613 crossovers during double-strand break repair in yeast. Cell. 2003;115: 401–11.
614 Available:
615 http://www.ncbi.nlm.nih.gov/pubmed/14622595%0Ahttp://www.pubmedcentral.nih.go

616 v/articlerender.fcgi?artid=PMC4493758

617 64. Urulangodi M, Sebesta M, Menolfi D, Szakal B, Sollier J, Sisakova A, et al. Local
618 regulation of the Srs2 helicase by the SUMO-like domain protein Esc2 promotes
619 recombination at sites of stalled replication. Genes Dev. 2015;29: 2067–2080.
620 doi:10.1101/gad.265629.115

621 65. Arbel M, Bronstein A, Sau S, Liefshitz B, Kupiec M. Access to pcna by srs2 and elg1
622 controls the choice between alternative repair pathways in saccharomyces cerevisiae.
623 MBio. 2020;11: 1–14. doi:10.1128/mBio.00705-20

624 66. Piberger AL, Bowry A, Kelly RDW, Walker AK, González-Acosta D, Bailey LJ, et al.
625 PrimPol-dependent single-stranded gap formation mediates homologous recombination
626 at bulky DNA adducts. Nat Commun. 2020; doi:10.1038/s41467-020-19570-7

627 67. Alexandrov LB, Nik-Zainal S, Wedge DC, Aparicio SAJR, Behjati S, Biankin A V., et
628 al. Signatures of mutational processes in human cancer. Nature. 2013;500: 415–421.
629 doi:10.1038/nature12477

630 68. Nik-Zainal S, Davies H, Staaf J, Ramakrishna M, Glodzik D, Zou X, et al. Landscape
631 of somatic mutations in 560 breast cancer whole-genome sequences. Nature. 2016;534:
632 47–54. doi:10.1038/nature17676

633 69. Nolan E, Savas P, Policheni AN, Darcy PK, Vaillant F, Mintoff CP, et al. Combined
634 immune checkpoint blockade as a therapeutic strategy for BRCA1-mutated breast
635 cancer. Sci Transl Med. 2017;9. doi:10.1126/scitranslmed.aal4922

636 70. Wen WX, Leong CO. Association of BRCA1- And BRCA2-deficiency with mutation
637 burden, expression of PD-L1/ PD-1, immune infiltrates, and T cell-inflamed signature
638 in breast cancer. PLoS One. 2019;14: 1–16. doi:10.1371/journal.pone.0215381

639 71. Taglialatela A, Leuzzi G, Sannino V, Cuella-Martin R, Huang J-W, Wu-Baer F, et al.
640 REV1-Polζ maintains the viability of homologous recombination-deficient cancer cells

641 through mutagenic repair of PRIMPOL-dependent ssDNA gaps. Mol Cell. 2021;81:
642 4008-4025.e7. doi:https://doi.org/10.1016/j.molcel.2021.08.016
643 72. Hurley D. In the Clinic. Neurol Today. 2017;17: 22–23.
644 doi:10.1097/01.nt.0000521902.81399.b2
645 73. Zhou J, Gelot C, Pantelidou C, Li A, Yücel H, Davis RE, et al. A first-in-class
646 polymerase theta inhibitor selectively targets homologous-recombination-deficient
647 tumors. Nat Cancer. 2021;2: 598–610. doi:10.1038/s43018-021-00203-x
648 74. Zatreanu D, Robinson HMR, Alkhatib O, Boursier M, Finch H, Geo L, et al. Polθ
649 inhibitors elicit BRCA-gene synthetic lethality and target PARP inhibitor resistance.
650 Nat Commun. 2021;12: 3636. doi:10.1038/s41467-021-23463-8
651 75. Wojtaszek JL, Chatterjee N, Najeeb J, Ramos A, Lee M, Bian K, et al. A Small
652 Molecule Targeting Mutagenic Translesion Synthesis Improves Chemotherapy. Cell.
653 2019;178: 152-159.e11. doi:10.1016/j.cell.2019.05.028
654 76. Baudin a, Ozier-Kalogeropoulos O, Denouel a, Lacroute F, Cullin C. A simple and
655 efficient method for direct gene deletion in Saccharomyces cerevisiae. Nucleic Acids
656 Res. 1993;21: 3329–3330. doi:10.1093/nar/21.14.3329
657 77. Longtine MS, McKenzie A, Demarini DJ, Shah NG, Wach A, Brachat A, et al.
658 Additional modules for versatile and economical PCR-based gene deletion and
659 modification in Saccharomyces cerevisiae. Yeast. 1998;14: 953–61.
660 doi:10.1002/(SICI)1097-0061(199807)14:10<953::AID-YEA293>3.0.CO;2-U
661 78. Sherman F. Getting started with yeast. Methods Enzymol. 2002;350: 3–41.
662 doi:10.1016/S0076-6879(02)50954-X
663 79. Ma CM, Coffey CW, DeWerd LA, Liu C, Nath R, Seltzer SM, et al. AAPM protocol
664 for 40-300 kV x-ray beam dosimetry in radiotherapy and radiobiology. Med Phys.
665 2001;28: 868–893. doi:10.1118/1.1374247

666 80. Spell RM, Jinks-Robertson S. Determination of mitotic recombination rates by
667 fluctuation analysis in Saccharomyces cerevisiae. Methods Mol Biol. 2004;
668

669 # Figure legend

670 **Fig 1. Rad55 plays a major role in UV-induced HR.** (A) Schematic representation of the
671 genetic system used. Frameshift mutations were introduced at the *Eco*RV site (RV, ±2 bp) or
672 the *Bgl*II site (Bg, +4 bp). HR between the two *ARG4* mutant alleles can restore a WT *ARG4*
673 allele associated with the [Arg+] phenotype. (B) Survival and (C) [Arg+] recombinant
674 frequencies after UV exposure of WT and *rad55*Δ diploid cells. (D) Survival and (E) [Arg+]
675 recombinant frequencies after γ irradiation of WT and *rad55*Δ diploid cells. (F) Spontaneous
676 mitotic [Arg+] recombinant rates ([Arg+] x 10^{-7} /cell/generation) of WT and *rad55*Δ diploid
677 strains.
678

679 **Fig 2. Channeling UV-induced DNA lesions into the *REV3*-dependent pathway in**
680 ***rad55*Δ cells.** (A) Survival of haploid cells following UV radiation. (B) Survival of diploid
681 cells following UV radiation. (C) UV-induced mutagenesis in WT and *rad55*Δ cells
682 determined by quantifying the Can^R mutant frequency for the indicated UV doses.
683

684 **Fig 3. Channeling UV-induced DNA lesions into the HR pathway in TLS-deficient cells.**
685 (A) UV-induced [Arg+] recombinant frequencies in WT and *rev3*Δ diploid cells. (B) UV-
686 induced [Arg+] recombinant frequencies in WT and *rad30*Δ diploid cells. (C) Survival of
687 diploid *rad30*Δ cells after UV radiation.
688

689 **Fig 4. *RAD55*-independent UV-induced HR in TLS-deficient cells.** (A) UV-induced
690 [Arg+] recombinant frequencies in *rad55*Δ *rev3*Δ diploid cells. The very strong UV

691 sensitivity displayed by the double mutant precluded the quantification of the UV-induced
692 recombinant rate at UV doses higher than 40J/m^2. (B) Survival of *rad55*Δ *rad30*Δ diploid
693 cells following UV radiation. (C) UV-induced [Arg+] recombinant frequencies in *rad55*Δ and
694 *rad30*Δ diploids cells. (D) Close-up view of (C) to exclude the hyper-recombinogenic
695 phenotype of *rad30*Δ. (E) *Rad55*Δ *mms2*Δ diploid cell-survival upon UV radiation. (F) UV-
696 induced [Arg+] recombinant frequencies in *rad55*Δ and *mms2*Δ diploid cells.
697
698 **Fig 5. Srs2 role in the *rad55*Δ mutant exposed to UV radiation.** (A) UV-induced [Arg+]
699 recombinant frequencies in *rad55*Δ *srs2*Δ diploid cells. (B) Close-up view of (A) to exclude
700 the hyper-recombinogenic phenotype of *srs2*Δ. (C) The acute UV sensitivity displayed by the
701 *rad55*Δ *rev3*Δ mutant is partially suppressed by *SRS2* deletion. The red arrow between the
702 *rev3*Δ *rad55*Δ and *rev3*Δ *rad55*Δ *srs2*Δ survival curves highlights the partial *srs2*Δ
703 suppression. (D) Survival curves of diploid cells following UV radiation. The acute
704 sensitivity to UV radiation of the diploid *srs2*Δ strain is suppressed by *rad55*Δ (blue arrow).
705
706 **Fig 6. TLS DNA polymerases are not required for cell survival after a site-specific DSB.**
707 (A) Schematic representation of the system used to measure repair of a HO-induced DSB by
708 gene conversion between ectopic copies of *MAT*. (B) Cell viability after DSB formation.
709
710 **Fig 7. Model of Rad55-Rad57 roles in the repair of ssDNA gaps by HR behind**
711 **replication forks.** The figure shows an ssDNA gap generated after stalling of a replicative
712 DNA polymerase at a UV-induced DNA lesion. This gap is a substrate for both the HR and
713 TLS pathways. (**A**) The three roles of the Rad55-Rad57 complex in Rad51 filament formation
714 on ssDNA gaps are highlighted: (1) formation of functional Rad51 filaments; (2) protection
715 against Srs2 dismantling activity; (3) prevention of TLS polymerase recruitment at the

716 primer/template junction. (**B**) In WT cells, Rad55-Rad57 heterodimers form and stabilize
717 Rad51 filaments on ssDNA leading to HR, avoiding bypass by TLS. Rad51 filaments could
718 prevent the recruitment of the TLS polymerases Polζ and Polη (collectively named TLS Pol)
719 by covering the 3' extremity blocked at the DNA lesion. (**C**) In the *rad55*Δ mutant, inefficient
720 and/or fewer Rad51 filaments are formed that cannot prevent the recruitment of the TLS
721 polymerases. Therefore, more UV-induced DNA lesions are channeled towards the TLS
722 pathway (red arrows). (**D**) In the *rev3*Δ or in the *rad30*Δ mutant, the absence of Polζ or Polη
723 allows channeling UV-induced DNA lesions towards the HR pathway (red arrows). (**E**) In the
724 *rad55*Δ *rev3*Δ and *rad55*Δ *rad30*Δ double mutants both the HR and the TLS pathways are
725 impaired.
726

727 # Supporting information

728 **S1 Fig. Rad57 plays a major role specifically in UV-induced HR.** (A) Survival, and (B)
729 [Arg+] recombinant frequencies in WT and *rad57*Δ diploid cells following UV radiation. (C)
730 Survival and (D) [Arg+] recombinant frequencies in WT and *rad57*Δ diploid cells after γ
731 irradiation.
732

733 **S2 Fig. Srs2 roles in the *rad57*Δ mutant exposed to UV radiation.** (A) UV-induced [Arg+]
734 recombinant frequencies in *rad57*Δ *srs2*Δ diploid cells. (B) Close-up view of (A) to exclude
735 the hyper-recombinogenic phenotype of *srs2*Δ. (C) Survival curves of diploid cells following
736 UV radiation. The acute sensitivity to UV radiation of the diploid *srs2*Δ strain is suppressed
737 by *rad57*Δ (blue arrow).
738

Figure 1

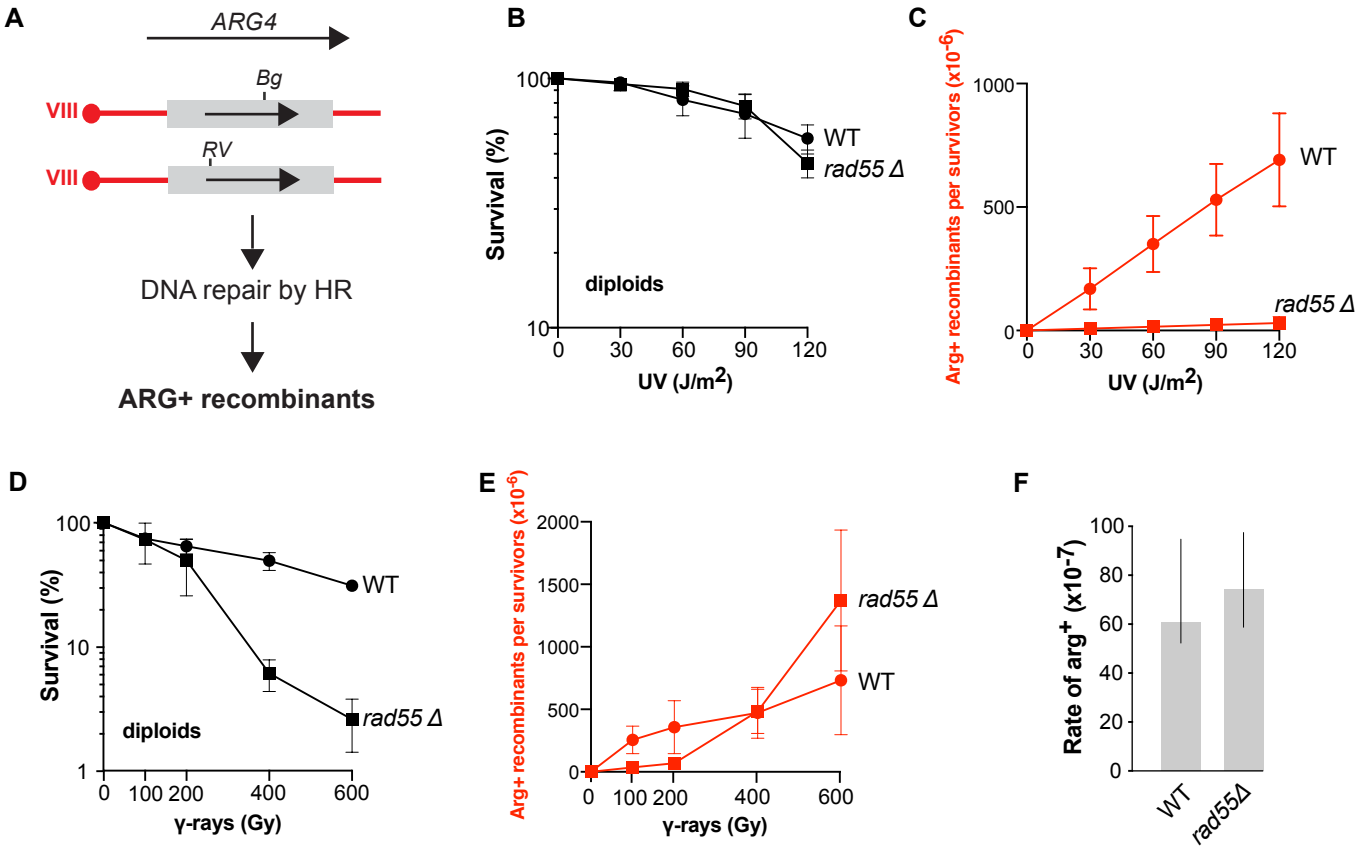
A
ARG4
Bg
VIII
RV
VIII
DNA repair by HR
ARG+ recombinants
B
Survival (%)
100
10
0
30
60
90
120
UV (J/m2)
WT
rad55 Δ
diploids
C
Arg+ recombinants per survivors (x10-6)
1000
500
0
0
30
60
90
120
UV (J/m2)
WT
rad55 Δ
D
Survival (%)
100
10
1
0
100
200
400
600
γ-rays (Gy)
WT
rad55 Δ
diploids
E
Arg+ recombinants per survivors (x10-6)
2000
1500
1000
500
0
0
100
200
400
600
γ-rays (Gy)
rad55 Δ
WT
F
Rate of arg+ (x10-7)
100
80
60
40
20
0
WT
rad55Δ

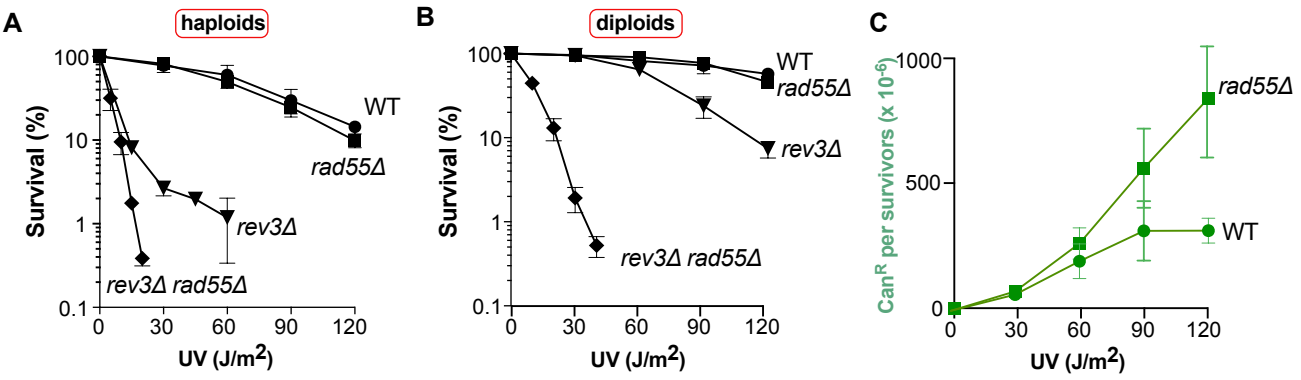
A
haploids
Survival (%)
100
10
1
0.1
0
30
60
90
120
UV (J/m2)
WT
rad55Δ
rev3Δ
rev3Δ rad55Δ
B
diploids
Survival (%)
100
10
1
0.1
0
30
60
90
120
UV (J/m2)
WT
rad55Δ
rev3Δ
rev3Δ rad55Δ
C
CanR per survivors (x 10-6)
1000
500
0
0
30
60
90
120
UV (J/m2)
rad55Δ
WT

Figure 2

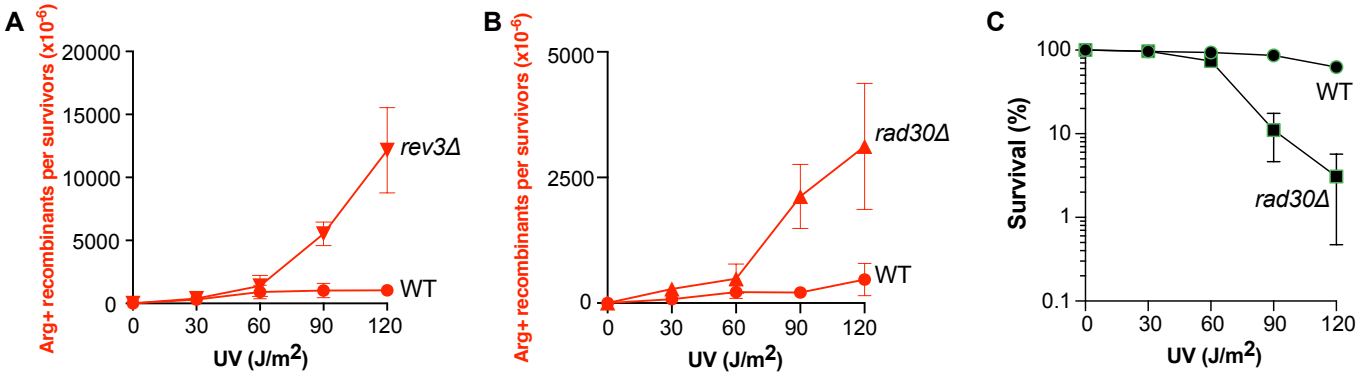
A
Arg+ recombinants per survivors (x10-6)
20000
15000
10000
5000
0
rev3Δ
WT
0
30
60
90
120
UV (J/m2)
B
Arg+ recombinants per survivors (x10-6)
5000
2500
0
rad30Δ
WT
0
30
60
90
120
UV (J/m2)
C
Survival (%)
100
10
1
0.1
WT
rad30Δ
0
30
60
90
120
UV (J/m2)

Figure 3

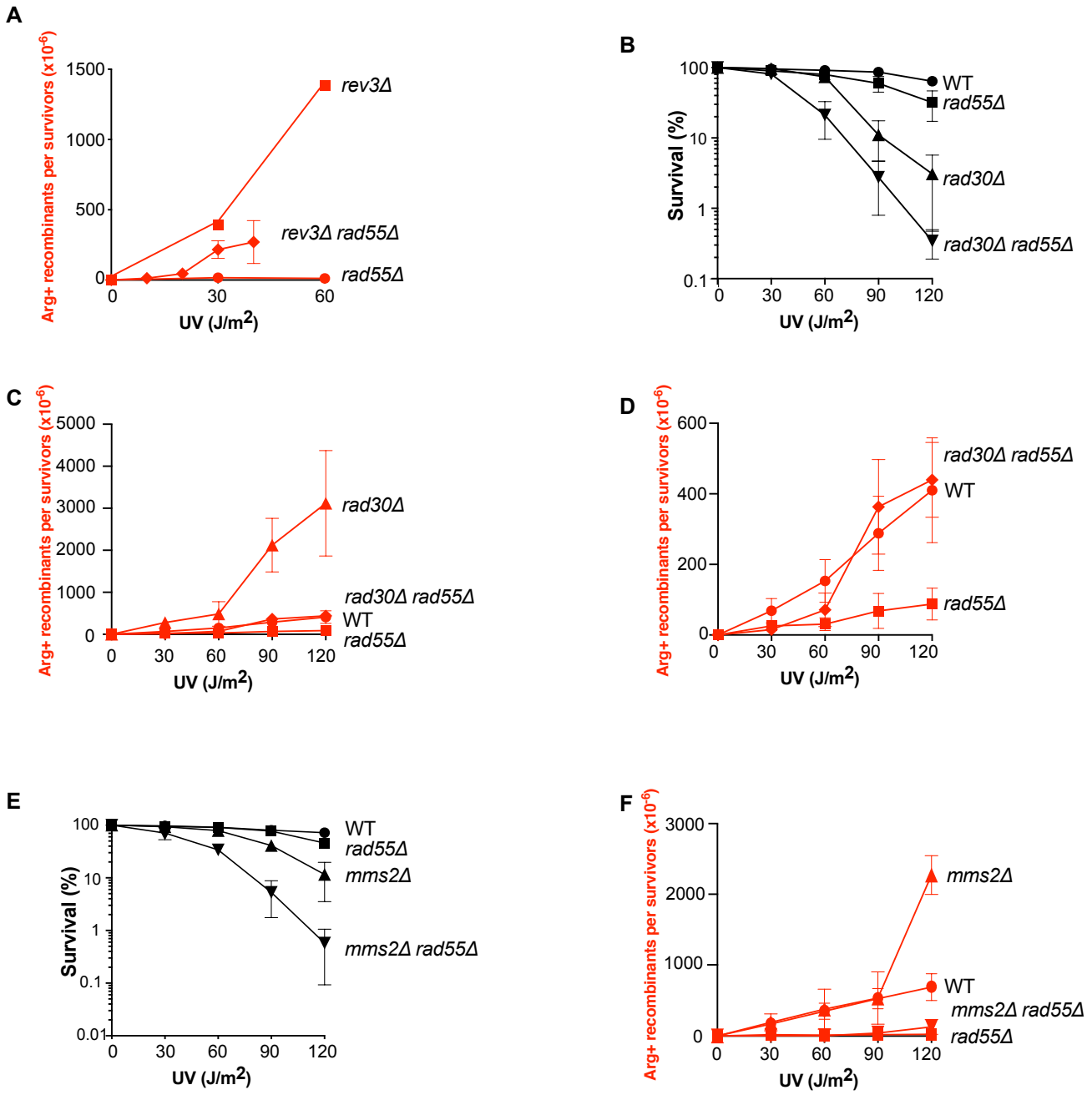
A
Arg+ recombinants per survivors (x10-6)
1500
1000
500
0
0
30
60
UV (J/m2)
rev3Δ
rev3Δ rad55Δ
rad55Δ
B
Survival (%)
100
10
1
0.1
0
30
60
90
120
UV (J/m2)
WT
rad55Δ
rad30Δ
rad30Δ rad55Δ
C
Arg+ recombinants per survivors (x10-6)
5000
4000
3000
2000
1000
0
0
30
60
90
120
UV (J/m2)
rad30Δ
rad30Δ rad55Δ
WT
rad55Δ
D
Arg+ recombinants per survivors (x10-6)
600
400
200
0
0
30
60
90
120
UV (J/m2)
rad30Δ rad55Δ
WT
rad55Δ
E
Survival (%)
100
10
1
0.1
0.01
0
30
60
90
120
UV (J/m2)
WT
rad55Δ
mms2Δ
mms2Δ rad55Δ
F
Arg+ recombinants per survivors (x10-6)
3000
2000
1000
0
0
30
60
90
120
UV (J/m2)
mms2Δ
WT
mms2Δ rad55Δ
rad55Δ

Figure 4

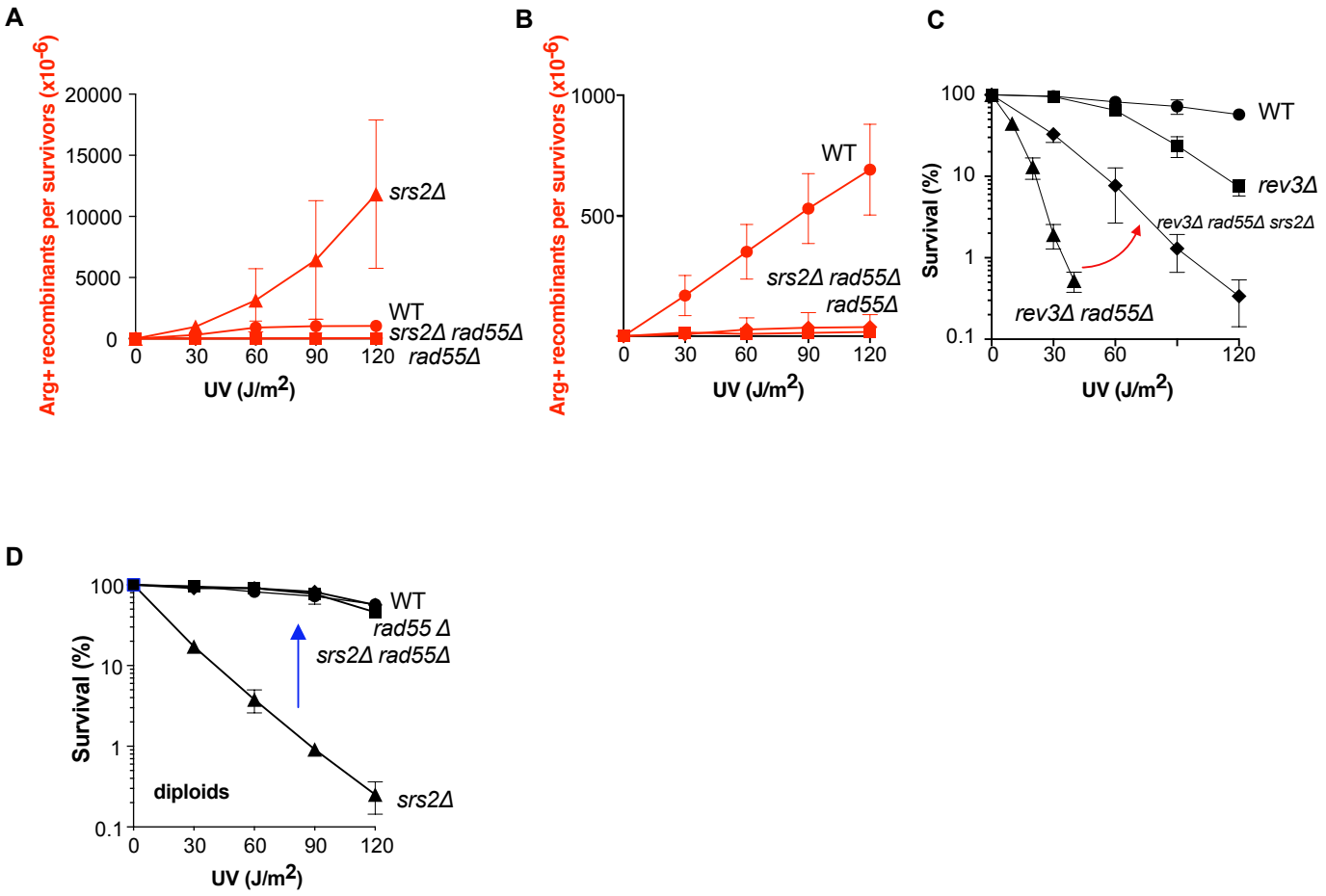
A
Arg+ recombinants per survivors (x10-6)
20000
15000
10000
5000
0
0
30
60
90
120
UV (J/m2)
srs2Δ
WT
srs2Δ rad55Δ
rad55Δ
B
Arg+ recombinants per survivors (x10-6)
1000
500
0
30
60
90
120
UV (J/m2)
WT
srs2Δ rad55Δ
rad55Δ
C
Survival (%)
100
10
1
0.1
0
30
60
120
UV (J/m2)
WT
rev3Δ
rev3Δ rad55Δ srs2Δ
rev3Δ rad55Δ
D
Survival (%)
100
10
1
0.1
0
30
60
90
120
UV (J/m2)
WT
rad55 Δ
srs2Δ rad55Δ
diploids
srs2Δ

Figure 5

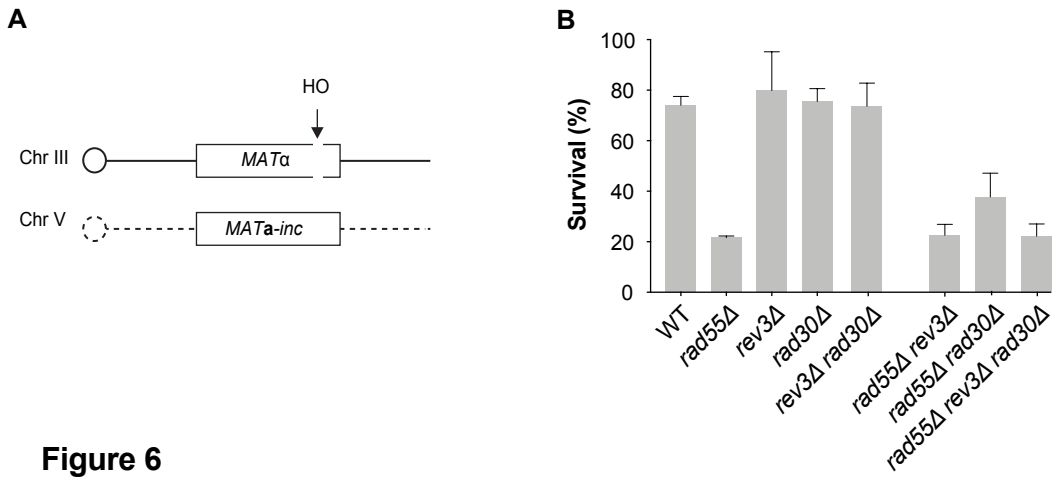
A
HO
Chr III
MATα
Chr V
MATa-inc
B
Survival (%)
100
80
60
40
20
0
WT
rad55Δ
rev3Δ
rad30Δ
rev3Δ rad30Δ
rad55Δ rev3Δ
rad55Δ rad30Δ
rad55Δ rev3Δ rad30Δ

Figure 6

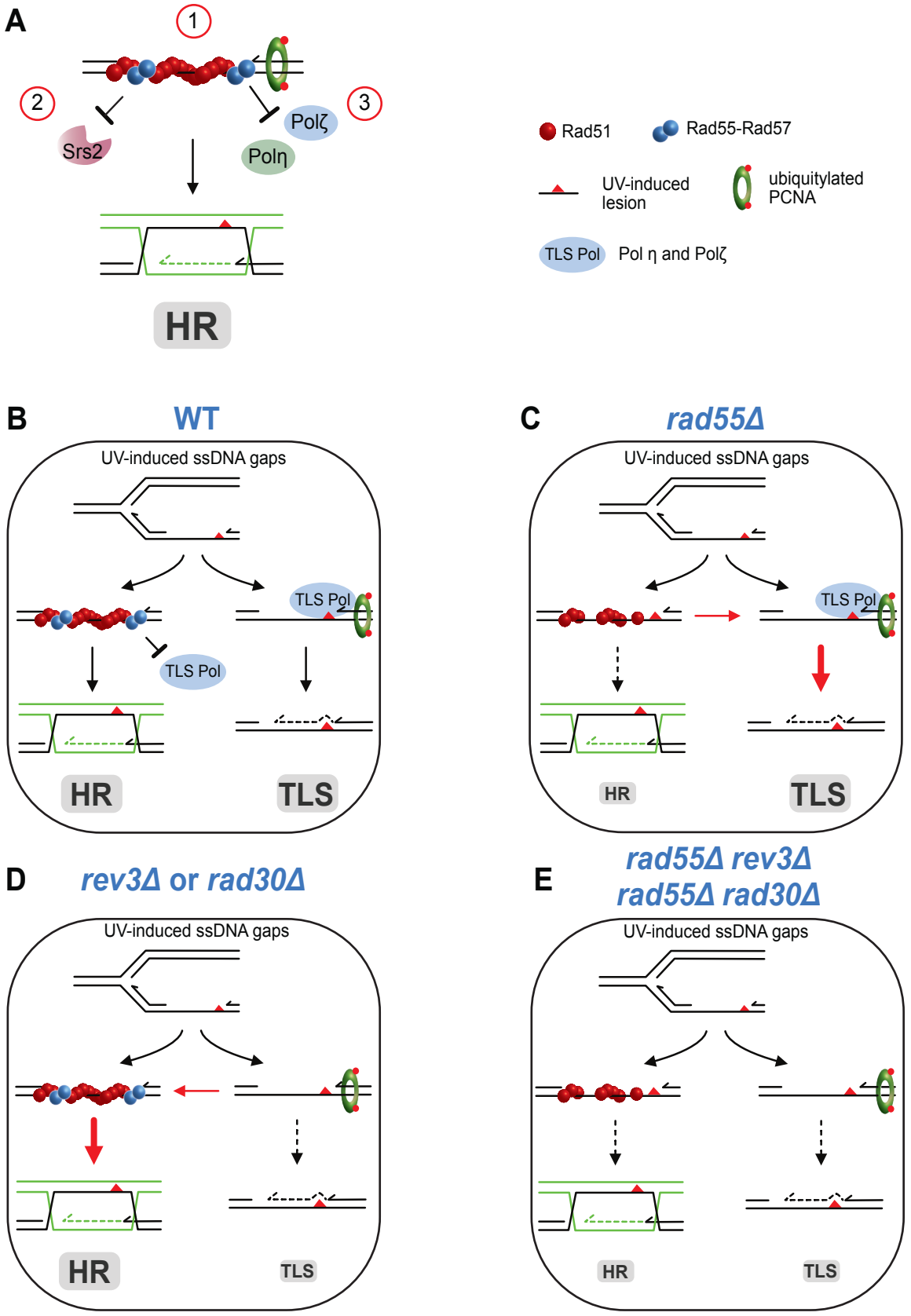
A
1
2
3
Srs2
Polζ
Polη
HR
Rad51
Rad55-Rad57
UV-induced lesion
ubiquitylated PCNA
TLS Pol
Pol η and Polζ
B
WT
UV-induced ssDNA gaps
TLS Pol
TLS Pol
HR
TLS
C
rad55Δ
UV-induced ssDNA gaps
TLS Pol
HR
TLS
D
rev3Δ or rad30Δ
UV-induced ssDNA gaps
HR
TLS
E
rad55Δ rev3Δ
rad55Δ rad30Δ
UV-induced ssDNA gaps
HR
TLS

Figure 7

Supplemental Figure S1

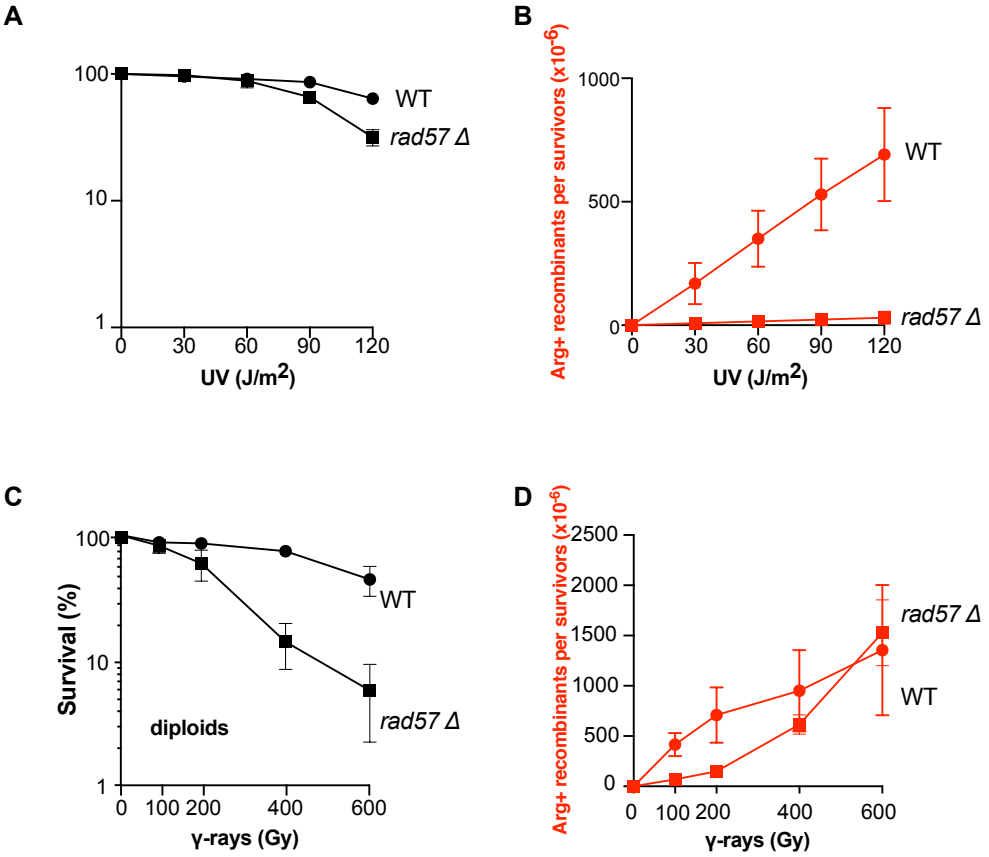

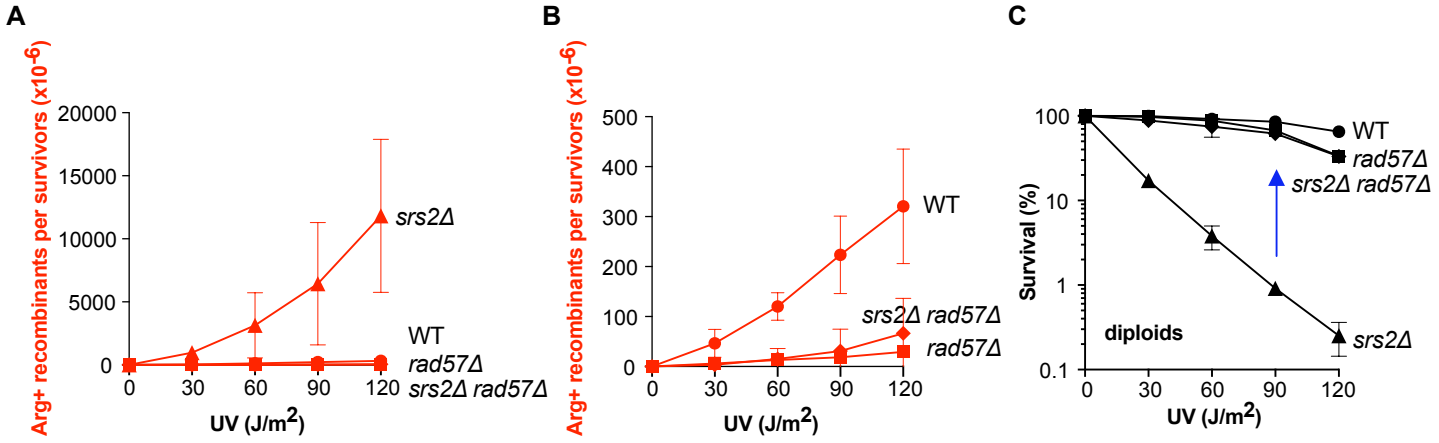

Supplemental Figure S2